

Inelastic excitation of ^{12}C and ^{14}N by 122 MeV protons and implications for the effective nucleon-nucleon interaction

J. R. Comfort

Department of Physics and Astronomy, University of Pittsburgh, Pittsburgh, Pennsylvania 15260

Sam M. Austin

Cyclotron Laboratory and Physics Department, Michigan State University, East Lansing, Michigan 48824

P. T. Debevec

Department of Physics, University of Illinois, Urbana, Illinois 61801

G. L. Moake*

Department of Physics, Purdue University, West Lafayette, Indiana 47907

R. W. Finlay

Department of Physics, Ohio University, Athens, Ohio 45701

W. G. Love

Department of Physics, University of Georgia, Athens, Georgia 30602

(Received 1 October 1979)

Cross sections for the $^{12}\text{C}(p,p')^{12}\text{C}$ and $^{14}\text{N}(p,p')^{14}\text{N}$ reactions have been measured at $E_p = 122$ MeV. Scattered protons were momentum analyzed in a dispersion-matched magnetic spectrograph and detected in a helical-cathode position-sensitive proportional counter. Transitions to states in ^{12}C at 4.44 MeV ($2^+, T=0$), 12.71 MeV ($1^+, 0$), 15.11 MeV ($1^+, 1$), 16.11 MeV ($2^+, 1$), and in ^{14}N at 2.31 MeV ($0^+, 1$) and 3.95 MeV ($1^+, 0$), are very useful for studying the spin-isospin dependence of the effective two-nucleon interaction. Cross sections for these states from the present experiment and from earlier measurements at 185 MeV have been analyzed in the distorted-wave impulse approximation. Simultaneous consideration of (e, e') data for the same transitions helped to disentangle some nuclear-structure and reaction-mechanism effects. The distorted-wave impulse approximation provides a good description of those transitions in ^{12}C mediated predominantly by the $S = T = 1$ part of the effective interaction and also gives a reasonable description of the $S = T = 0$ transitions in both nuclei. The mechanisms for excitation of the 12.71-MeV state in ^{12}C ($S = 1, T = 0$) and the 2.31-MeV state in ^{14}N ($S = 1, T = 1$) remain a puzzle.

[NUCLEAR REACTIONS $^{12}\text{C}, ^{14}\text{N}(p, p'), (p, p'), E = 122$ MeV; measured $\sigma(E_p, \theta)$; resolution 100 keV; $\theta = 6-60^\circ$. ^{12}C 2^+ states deduced β_2 DWIA analysis; microscopic effective interaction with $\vec{L} \cdot \vec{S}$, tensor, and exchange terms.]

I. INTRODUCTION

A fundamental goal of nuclear physics is to relate nuclear structure and reaction dynamics to the underlying nucleon-nucleon ($N-N$) interaction. Since this interaction is complicated and has other awkward features such as a strong short-range repulsion, it is necessary in practice to represent it by an effective interaction V^{eff} . This in turn must be tested and understood before nucleon-nucleus scattering can be used as a detailed probe of nuclear structure.

One approach to this might be the construction of complex optical-model potentials from realistic internucleon interactions and the comparison of predicted cross sections with the extensive body of elastic-scattering data. Although these procedures have received considerable impetus recently from the work of several groups,^{1,2} they have the limitation that elastic scattering is not

selectively sensitive to each individual spin and isospin component of the effective interaction.

On the other hand, inelastic-scattering and charge-exchange reactions have the advantage, particularly on light nuclei, that selection rules and reaction dynamics often isolate a very few components of V^{eff} . Bertsch *et al.*³ have constructed a V^{eff} based on the shell-model G matrix and this has been applied with generally satisfactory results to nucleon data for energies less than 65 MeV.^{3,4} Since the effective interaction is energy dependent,⁴ complementary studies at different energies or for different ranges of momentum transfer will therefore enrich our understanding of its components and also of nuclear structure.

In many ways intermediate energies such as 100–200 MeV seem superior for such studies. Resolution is still sufficient to permit separation of many states of interest. The reaction dynamics should also be considerably simpler since the im-

portance of multistep processes⁵ and resonances⁶ should be reduced and sensitivity to optical distortions will be smaller. It is unfortunate that little is known about the effective interaction in this energy range.

To the extent that the distorted-wave impulse approximation (DWIA) is applicable, V^{eff} is related simply to the free nucleon-nucleon interaction.⁷ But the DWIA is not unquestionably valid near 100 MeV and only a few tests of its adequacy have been made. Moreover, as we shall see, empirical procedures for fixing V^{eff} are not useful at these energies. The present study attempts to delineate the range of validity of the impulse approximation and to test a microscopic effective interaction constructed for this energy range.

Inelastic nucleon scattering from ^{12}C and ^{14}N provides an excellent situation for studying these issues. States are available which isolate most individual combinations of spin and isospin transfer and some which are also particularly sensitive to the tensor force. Moreover, shell-model wave functions are available for these states which reproduce many of the known properties quite well. Since isospin is a rather good quantum number for these light nuclei, the charge form factor, which is determined rather well from high-quality (e, e') data, is a good measure of both proton and neutron transition densities. Although the large oblate deformation of ^{12}C is often thought to create unusual difficulties in interpretations of data, it is found here that the problems are not very severe and that ^{12}C is indeed a tractable nucleus.

This paper reports measurements of (p, p') reactions on ^{12}C and ^{14}N at an energy of 122 MeV. Attention is focused on transitions to states that correspond to rearrangements of the $1p$ -shell nucleons. In ^{12}C these are the 2^+ state at 4.44 MeV ($T=0$) and 16.11 MeV ($T=1$), and the 1^+ states at 12.71 MeV ($T=0$) and 15.11 MeV ($T=1$). In ^{14}N the transitions are from the 1^+ ($T=0$) ground state to the 0^+ ($T=1$) state at 2.31 MeV and the 1^+ ($T=0$) state at 3.95 MeV. This selection spans the full range of terms in V^{eff} , often with strong constraints on the number of significant components. For example, the 15.11-MeV transition ($S=T=1$) can be expected to be particularly sensitive to the one-pion-exchange (OPE) part of the N - N interaction. The direct contributions to the other transitions in ^{12}C might be more sensitive to the exchange of mesons of larger mass and other aspects of the short-range N - N interaction.

After a brief phenomenological interpretation of the data, analysis will be made in terms of a thoroughgoing treatment of an effective interaction derived from elastic N - N data at 140 MeV and applied in the DWIA. In order to study the energy

dependent of V^{eff} , analysis is also made of data near 185 MeV taken from the literature.^{8,9}

Studies similar to this have been carried out in the past.¹⁰⁻¹³ Our approach is somewhat more *a priori*. We take the wave functions, the effective interaction, and reaction dynamics as known and inquire how well the data are reproduced. Auxiliary studies on some of these items allow us to reach specific conclusions regarding the components of V^{eff} .

II. EXPERIMENTAL PROCEDURES

A. Data acquisition

A beam of 122-MeV protons from the Indiana University cyclotron bombarded targets of ^{12}C and ^{14}N placed in a 61-cm-diameter scattering chamber. The ^{12}C target was of natural graphite with a thickness of 11.3 mg/cm², while the ^{14}N target consisted of about 5.8 mg/cm² of melamine evaporated onto backings of formvar and carbon with a thickness of 25 $\mu\text{g}/\text{cm}^2$. A thick BN target (26.9 mg/cm²) was used to check the normalization of the ^{14}N data.

Emerging protons were momentum analyzed in a quadrupole-dipole-dipole-multipole magnetic spectrograph operating in a dispersion-matched mode and were detected in a helical-cathode, position-sensitive proportional chamber.¹⁴ This chamber was followed by two plastic scintillator detectors of thicknesses 0.63 and 1.27 cm which were used for particle identification. The solid angle of the spectrograph was about 1.5 msr ($\pm 0.5^\circ$ horizontally) at forward angles and 2.58 msr ($\pm 1.0^\circ$) for larger angles. For some of the elastic scattering data, solid angles a factor of 10 smaller were used at the forward angles.

The position of a particle in the focal plane was determined from the time difference of signals from the two ends of the helical-cathode wire. Upon a triple coincidence between the helix and the two scintillators, the position signal and the signals from the scintillators E_1 and E_2 were passed through an ADC system and processed by the program DERIVE¹⁵ in an on-line computer. Protons were selected digitally by imposing a contour on a two-dimensional E_1 vs E_2 display. The dead time of the system was monitored by feeding pulser signals triggered from the current integrator through the entire system. Event rates were kept to a few hundred per second and the corresponding dead times were only a few percent. The relative efficiency of the helix across its length was checked and monitored. The overall energy resolution was typically 80–100 keV.

Special care was taken with the data acquisition for ^{14}N . The state of principal interest lies low

in excitation energy at 2.31 MeV and has a very small cross section. Backgrounds were consequently a severe problem for small angles. Background from a small beam halo was eliminated by stacking several empty frames to the rear of the target, thus degrading the halo protons below the energy range of interest. At forward angles, it was not feasible to have the elastic and 2.31-MeV peaks on the detector simultaneously. Yet moving the elastic group off the end of the detector produced additional backgrounds. A thick lead block placed in front of the focal plane at the position of the elastic group generated no spurious events and, together with the thick target holder, allowed reliable data to be taken at angles as small as 6° . An additional problem was the fragility of the melamine target. Beams were therefore kept low and possible target deterioration was monitored by numerous measurements at 14° .

B. Data reduction for ^{12}C

Because of the small energy bite of the spectrograph, it was necessary to take data at two different magnetic field settings. One group included elastic scattering and inelastic scattering to the 4.44-MeV state, and the other spanned the region of excitation from about 10 to 17 MeV. Spectra for the two groups at a laboratory angle of 39° are shown in Fig. 1. Data were not obtained for the states at 7.65 and 9.64 MeV.

Analysis of the data in the first group was straightforward. In the higher excitation-energy group, the narrow states of interest sat upon a continuum resulting from both three-body breakup and other broad states. Yields were determined by representing the continuum under them by smooth curves. After they were subsequently removed from the data, the resultant spectra were

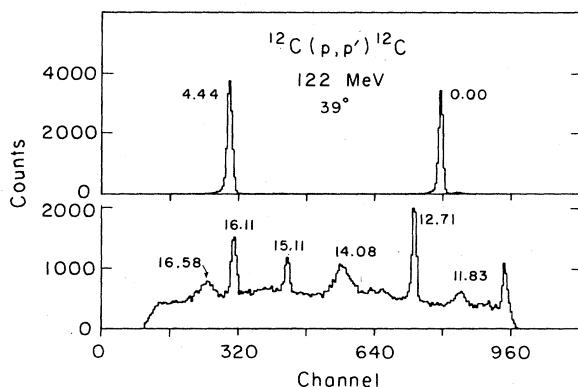


FIG. 1. Representative spectra of the $^{12}\text{C}(p, p')^{12}\text{C}$ reaction at two separate field strengths of the magnetic spectrograph. Peaks are labeled with their excitation energies.

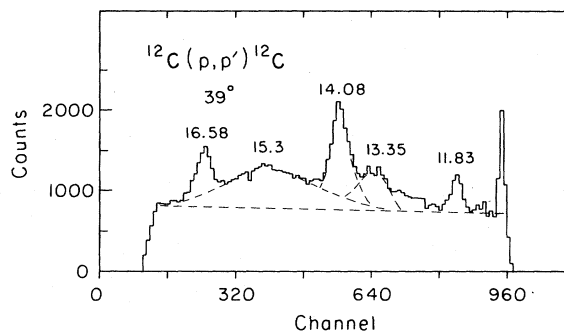


FIG. 2. Compressed spectrum of ^{12}C for the excitation-energy range 11–17 MeV. Three narrow peaks have been removed (see Fig. 1). The dotted lines indicate the “backgrounds” assumed for the remaining peaks.

compressed. This enhanced the visibility of broader states, which were similarly extracted. Figure 2 shows the compressed spectrum at 39° and the assumed “backgrounds.”

The center-of-mass differential cross sections (relativistic kinematics) for all states are shown in Figs. 3 and 4. The elastic cross sections in Fig. 3 have been corrected for the approximate 1.5% unresolved contribution from ^{13}C at forward angles. Data were obtained on two separate occasions. The absolute cross sections for several repeat runs reproduced very well within statistics, apart from an overall scale change of about 4%. This was attributed to a change in Faraday cups. The final cross sections for ^{12}C were normalized according to the experience at IUCF, for which 1–2% agreement with the absolute cross sections

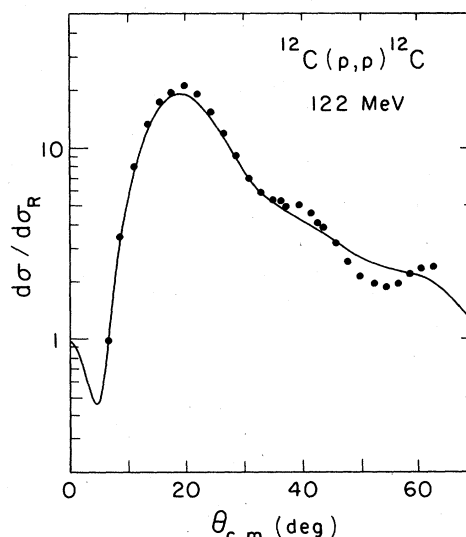


FIG. 3. The angular distribution for the scattering of 122-MeV protons from ^{12}C , in ratio to the Rutherford cross section (relativistic kinematics only).

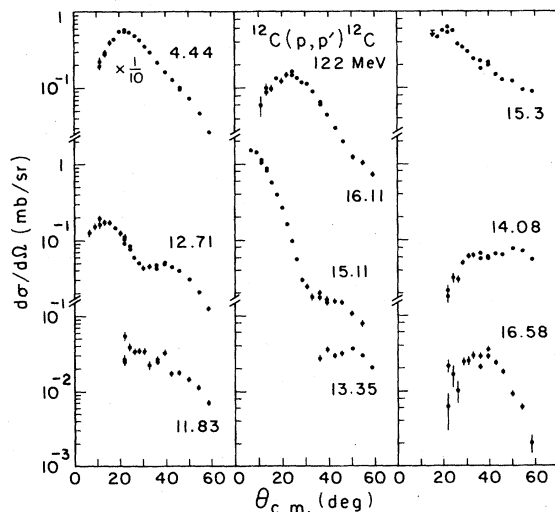


FIG. 4. Differential cross sections for the states of ^{12}C seen in the (p, p') reaction. The excitation energy of each state is indicated. Error bars are shown when they exceed the size of the data points.

of calibration reactions is normally obtained.¹⁶ The absolute scale is believed to be reliable to better than 4%.

No effort has been made to interpret the data for states other than those enumerated earlier. Most have known J^π assignments.¹⁷ The broad state at 15.3 MeV has been reported previously and interpreted^{18,19} as having $J^\pi = 2^+, T = 0$.

C. Data reduction for ^{14}N

A representative spectrum for $^{14}\text{N}(p, p')^{14}\text{N}$ is shown in Fig. 5. Angular distributions were extracted for the ground state and the excited states at 2.31 and 3.95 MeV. States at higher excitation energies are obscured by impurity peaks at many angles. The angular distributions for scattering

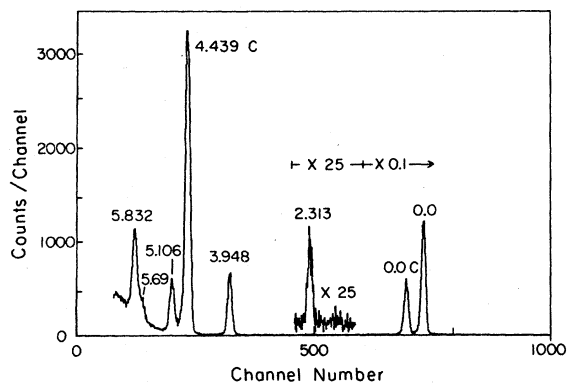


FIG. 5. Composite spectrum of protons scattered from a melamine target at 26° . Peaks labeled C are from the ^{12}C component of the target and the remainder are from ^{14}N .

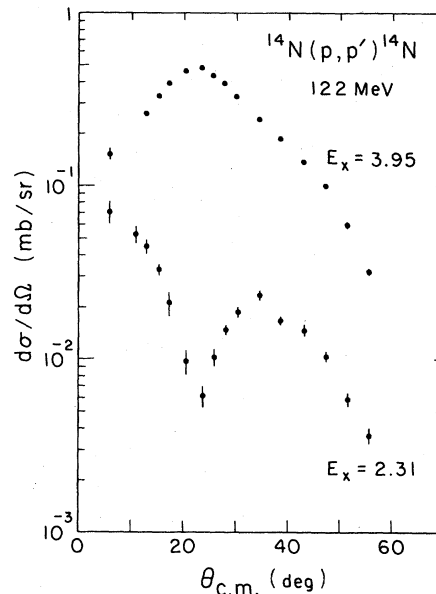


FIG. 6. Differential cross sections for (p, p') reactions to excited states of ^{14}N .

from ^{14}N , shown in Fig. 6, were normalized to the cross sections for $^{12}\text{C}(p, p')^{12}\text{C}$ (4.44 MeV) by using the data of Fig. 4. The yields for this state were observed simultaneously with that for the ^{14}N states upon bombardment of the melamine target. The normalization constant was compared at 28° to an absolute cross-section scale determined by use of a thick BN target. The two normalizations agreed to within 2%. Effects of deterioration of the melamine target were less than $\pm 3\%$. The overall cross-section scale is believed accurate to within $\pm 5\%$. A tabulation of all the cross sections has been deposited in the Physics Auxiliary Publications Service.²⁰

III. COLLECTIVE MODEL INTERPRETATION

Since collective models have been applied frequently to the excitation of ^{12}C , it is useful for orientation purposes to make brief comparisons with the data here. Although the focus of our study is on microscopic interpretations, the underlying intent of this section is to help gauge the relative importance of various contributions. The parameters for the optical-model potential describing 122-MeV proton scattering from ^{12}C were obtained in a companion study²¹ and are listed in Table I. The fit to the elastic-scattering data is shown in Fig. 3.

A direct application of the conventional collective model to the excitation of the $2^+ T = 0$ state at 4.44 MeV gave agreement with the maximum cross section near 20° for a deformation parameter $|\beta_2|$

TABLE I. The optical potentials used in the calculations. The potentials are defined by $U(r) = V_C(r) + V_F(r) + iWf_I(r) + V_{so}(1/r)(d/dr)f_{so}(r)\vec{l} \cdot \vec{s}$, where V_C is the coulomb potential for a uniformly charged sphere $f_i(r) = 1/(1 + e^{x_i})$ and $x_i = (r - R_i)/a_i$ with $R_i = r_i A^{1/3}$. Energies have units MeV and lengths have units fm. The potentials are defined for use with relativistic kinematics (see Ref. 21).

Particle	Energy	V	r_R	a_R	W	r_I	a_I	V_{so}	r_{so}	a_{so}	r_c
<i>p</i>	122	-18.3	1.20	0.65	-10.6	1.30	0.64	-18.3	0.90	0.50	1.2
<i>p</i>	183	-12.5	1.20	0.68	-13.1	1.20	0.61	-16.4	0.90	0.49	1.2
<i>d</i>	110	-68.0	1.20	0.62	-14.4	1.40	0.67	-11.0	0.90	0.50	1.2

= 0.55. At larger angles the calculated curve fell off much too steeply. When corrections for Coulomb excitation and the deformation of the spin-orbit potential were included, the value was reduced to $|\beta_2| \approx 0.45$. The deformed spin-orbit potential also enhances the cross sections at the larger angles. It is interesting to note that when the Woods-Saxon potentials themselves were deformed and the monopole part projected out, the best fit to the elastic-scattering data was achieved for a value $\beta_2 = -0.44$.

We may thus anticipate that at 122 MeV the Coulomb and spin-orbit interactions may each make about 10% corrections to the $2^+ T=0$ transition intensities and that the latter interaction may be quite important for producing correct shapes at large angles. In the same model, but without the corrections, the transition to the $2^+ T=1$ state at 16.11 MeV requires a value $|\beta_2| = 0.085$.

The transitions to the 1^+ states may proceed by $L=0$ and 2. The collective model allows the $L=0$ part to have both volume and surface-derivative terms.²² Satchler found that the $L=2$ parts were dominant for both the 12.71- and 15.11-MeV transitions in ^{12}C induced by 46-MeV protons.²² This could raise serious problems in the present study. Since the central terms of the microscopic effective interaction produce negligible $L=2$ contributions, their dominance would have to result from the tensor interaction. The sensitivity to the important central terms then might well be lost.

We find, however, that the situation is not so disturbing at 122 MeV. In fact, both the 12.71- and the 15.11-MeV states may be fitted (out to about 30°) with combinations of only the volume and surface $L=0$ terms. The combinations did not preserve the volume integral of the potential, but oscillations of the diffuseness parameters²² were not included. The situation is ambiguous since alternative combinations with $L=2$ contributions were also possible. However, in all cases, the $L=0$ terms were the dominant ones, especially for the 15.11-MeV transition. Some reasons relating to reaction dynamics are offered in the companion article²¹ for the difficulties at 46 MeV.

IV. MICROSCOPIC DWIA CALCULATIONS

A. The effective interaction

It has been suggested¹⁰ that above ~ 100 -MeV proton bombarding energy, the distorted-wave impulse approximation might be appropriate for interpreting nucleon-nucleus scattering. In the DWIA, V^{eff} is taken to be the free N - N t matrix. When valid, the appeal of this approach is evident; V^{eff} may be regarded as known and attention can be focused directly on extracting nuclear structure information. The objective of this section is to assess empirically the validity of this approach for a variety of nuclear transitions.

The use of the DWIA implies that the effects of multiple scattering and multistep contributions are either negligible or are well described by the distorted waves. In a companion study²¹ it was found that, for relatively strong transitions, the effects of a number of strong multistep processes are accurately included in one-step calculations provided that one uses optical-model parameters that reproduce the elastic scattering in a single-channel approximation. Additional discussion of multistep processes is given in Sec. VB.

The two-nucleon interaction may be written

$$V_{12}^{eff} = V_{12}^{central} + V_{12}^{spin-orbit} + V_{12}^{tensor}, \quad (1)$$

where in more detail

$$V_{12}^{cent} = V_0 + V_\sigma \vec{\sigma}_1 \cdot \vec{\sigma}_2 + V_\tau \vec{\tau}_1 \cdot \vec{\tau}_2 + V_{\sigma\tau} (\vec{\sigma}_1 \cdot \vec{\sigma}_2) (\vec{\tau}_1 \cdot \vec{\tau}_2), \quad (2a)$$

$$V_{12}^{so} = (V_{LS} + V_{LS\tau} \vec{\tau}_1 \cdot \vec{\tau}_2) \vec{L} \cdot \vec{S}, \quad (2b)$$

$$V_{12}^{ten} = (V_T + V_{T\tau} \vec{\tau}_1 \cdot \vec{\tau}_2) S_{12}. \quad (2c)$$

S_{12} is the tensor operator

$$S_{12} = 3(\vec{\sigma}_1 \cdot \hat{r}_{12})(\vec{\sigma}_2 \cdot \hat{r}_{12}) - \vec{\sigma}_1 \cdot \vec{\sigma}_2. \quad (3)$$

All interaction strengths are functions of the relative coordinate \vec{r}_{12} . For these we use the complex local coordinate-space representation of the antisymmetrized on-shell t matrix reported in Refs. 4 and 23. This V^{eff} basically consists of a sum of Yukawa terms with the three ranges

(0.25, 0.4, and 1.414 fm) chosen to reflect the exchange of various mesons. The tensor part of V^{eff} has an $r^2 X$ Yukawa form and the maximum (third) range is 0.7 fm. The specific interaction was constructed from the N - N scattering phase shifts at 140 MeV,²⁴ an energy that is intermediate to the two cases considered here. The constraint was imposed that only the $V_{\sigma\tau}$ interaction has a term with the longest range, corresponding to one-pion exchange. This and the limitation on the number of ranges are the main differences between this interaction and that of Picklesimer and Walker.²⁵

A rough criterion for neglecting knockon exchange terms is that $kR \gg 1$ where k is the incident momentum in fm^{-1} and R denotes each of the ranges. When this condition is met, V^{eff} is incapable of transferring the required momentum with appreciable amplitude. For the bombarding energies considered here, $k \sim 2-3 \text{ fm}^{-1}$ so that exchange terms may be expected to be important for the short-range parts of V^{eff} . The exchange contributions were calculated exactly with a modified version of the code DWBA70.²⁶ Relativistic kinematics was also used. The appropriate optical potentials are given in Table I.

The remainder of this section describes the calculations based on shell-model wave functions and the effective interaction in the DWIA. The single-particle wave functions for the bound particles were of harmonic-oscillator form with an oscillator parameter chosen to match the prominent maxima of the longitudinal and transverse form factors $F_L(q)$ and $F_T(q)$, respectively, obtained from (e, e') experiments.²⁷ The parameters for the various transitions are listed in Table II. Wave functions constructed from Woods-Saxon potentials may also be used. The results are generally rather insensitive to this choice, as well as to reasonable variations of the Woods-Saxon parameters and binding energies.

B. Shell-model wave functions

One of the best shell-model descriptions for the states of ^{12}C and ^{14}N is provided by the effective

TABLE II. The parameters for the harmonic-oscillator bound-state wave functions, where the $l=0$ radial dependence is given by $\sim \exp(-\frac{1}{2}\mu^2 r^2)$.

Nucleus	Final state	μ (fm^{-1})
^{12}C	4.44	0.568
	12.71	0.609
	15.11	0.513
	16.11	0.610
^{14}N	2.31	0.588
	3.95	0.595

1p-shell interaction of Cohen and Kurath (CKWF).²⁸ The wave functions for ^{12}C and ^{14}N were constructed from the (8-16) POT and (8-16)2BME two-body matrix elements, respectively. For the 2.31-MeV transition in ^{14}N we considered as an alternative the wave functions determined by Ensslin *et al.*²⁹ directly from (e, e') form factors and other experimental data.

The most simple view of ^{12}C is that the $p_{3/2}$ orbit is entirely filled and that the 2^+ and 1^+ states with $T=0$ and 1 are formed by promoting a single nucleon to the $p_{1/2}$ orbit. However, for the CKWF, the ground state has a population probability of about 6.5 $p_{3/2}$ particles, as do also the excited states (the 16.11-MeV state actually contains about 6.7 $p_{3/2}$ particles). The main components of the transition amplitudes involve both $p_{3/2} \rightarrow p_{1/2}$ and $p_{1/2} \rightarrow p_{3/2}$ transitions. The effect on the (p, p') cross sections is illustrated in Fig. 7. These were calculated for a simple Yukawa interaction of 1 fm range. It is clear that a good description of the wave functions is essential. The main limitation of the CKWF is the truncation to the 1p shell so that the collective effects on the transitions will be underestimated.

C. The $T=1$ states of ^{12}C

1. The 1^+ state at 15.11 MeV

Since this state has unnatural parity and $T=1$, its excitation is mediated primarily by the $V_{\sigma\tau}$ part of V^{eff} whose origin is largely the OPE interaction. Figure 8 shows a comparison of the experimental data at 122 MeV and the DWIA calculations. Since both the peak value of $|F_T(q)|^2$ and the ground-state $M1$ radiative width¹⁷ are under-

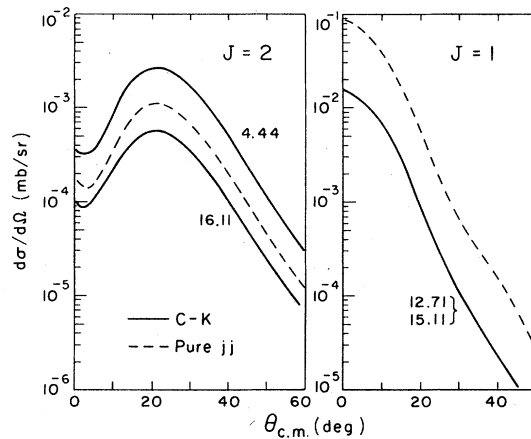


FIG. 7. Cross sections of four states in ^{12}C for the (p, p') reaction at 122 MeV resulting from pure single-particle $p_{3/2} \rightarrow p_{1/2}$ transitions and from the Cohen-Kurath wave functions. The dashed curves for each J apply to both transitions and the CK curves for $J=1$ agree.

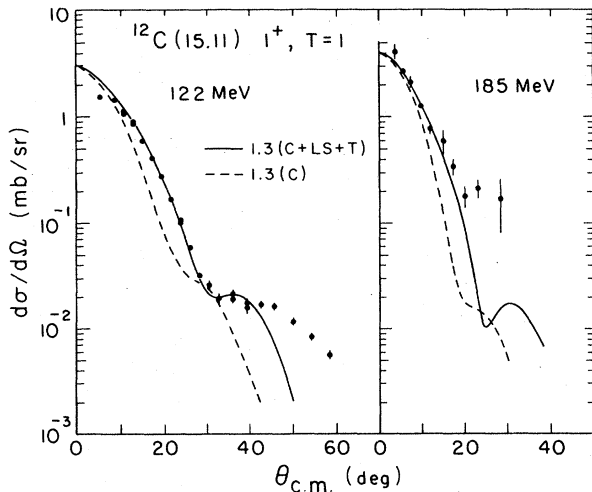


FIG. 8. DWIA calculations for the 15.11-MeV transition in ^{12}C at two proton energies in comparison with the data. The calculations include central (C), spin-orbit (LS), and tensor (T) contributions and are renormalized by a multiplicative factor of 1.3.

estimated by a factor of about 1.3 by the CKWF, the calculated cross sections have been multiplied by 1.3. It may be noted, however, that the CKWF give the correct value of the ft value from β decay which, like the (p, p') reaction, is dominated by the spin contribution. The dashed curve is for the central part of the force only; the solid curve includes contributions from central, spin-orbit, and tensor terms. The two-body spin-orbit interaction has a weak isovector part and is therefore unimportant for this cross section. When the tensor force is included the results are quite satisfactory; without it, the shape of the calculated cross section is in much poorer agreement with the data.

The results are especially significant when one notes that the transverse form factor given by the CKWF agrees well in shape with that inferred from (e, e') measurements²⁷ out to momentum transfers of $q \sim 1.5 \text{ fm}^{-1}$, which for 122-MeV protons corresponds to $\sim 37^\circ$. A second peak²⁷ in $|F_T(q)|^2$ near 2 fm^{-1} is very poorly described by these wave functions and this deficiency shows up in the predicted (p, p') results. It seems fairly clear that the $S=T=1$ part of V^{eff} is given reliably by the free $N-N$ t matrix as represented in Refs. 4 and 23, at least out to $q \sim 1.5 \text{ fm}^{-1}$.

Analogous calculations have been made at 185 MeV and these are compared with experimental data from Ref. 8 in Fig. 8. As at 122 MeV, the tensor force significantly improves the shape of the calculated cross section. It is somewhat disturbing that the shape is correctly predicted out to only $q \sim 0.8 \text{ fm}^{-1}$. Modern and more complete data

for this OPE dominated transition would be desirable. The disagreement at 185 MeV might also reflect the greater departure in energy from that of the 140-MeV t matrix being used.

2. The 2^+ state in ^{12}C at 16.11 MeV

Excitation of this state is in principle more complicated than for the 1^+ state since both the V_T and $V_{\sigma T}$ terms may contribute, in addition to the V_{LS_T} and V_{T_T} terms. The isovector part of the spin-orbit force is small and thus V_{LS_T} contributes relatively little. Also, at intermediate energies, $V_{\sigma T}$ is more important than V_T , so that the $S=1$ contributions are at least as large as those for $S=0$. Since the tensor contributions remain large, we are sensitive mainly to the same terms of V^{eff} as for the 1^+ state.

The wave function for this state is somewhat uncertain. The $S=1$ part of the transition density is sampled by $F_T(q)$ in (e, e') experiments. Unfortunately the shape of $|F_T(q)|^2$ is not reproduced in detail by the CKWF.²⁷ While the magnitude is properly given for small q , the theoretical result must be reduced by a factor ~ 0.7 in order to match the experimental value at the peak. The relationship of the experimental and theoretical ground-state widths of this state is also unclear. The CKWF estimate is in reasonable agreement with one recent measurement³⁰ and a factor of 2 larger than another.³¹ In any case, such a discrepancy would not be as serious as it might initially appear because the radiative decay is isovector $E2$ whereas the (p, p') reaction proceeds mainly by the $S=T=1$ terms.

Figure 9 shows a comparison of the 122-MeV data and the DWIA calculations, the latter scaled

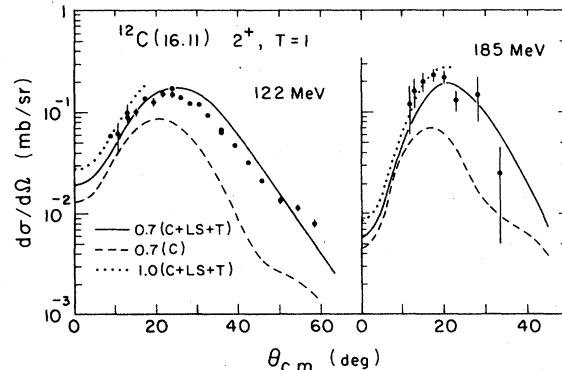


FIG. 9. Comparison of DWIA calculations with data for the 16.11-MeV transition in ^{12}C . See also the caption for Fig. 8. The curves have been renormalized by 0.7 except for the dotted curves where unit normalization for low momentum transfer is also shown.

down by a factor 0.7 corresponding to use of the CKWF for large q . Again the tensor part is very important in establishing the proper magnitude and the spin-orbit part improves the shape at larger angles.

Similar calculations have been made at 185 MeV and are compared with experimental data⁸ in Fig. 9. The data at this energy are much less definitive than those at 122 MeV due to the larger errors and the much smaller range of momentum transfers. The calculated cross sections would appear to need no renormalization, corresponding to the predictions of the CKWF at low q .²⁷ At both energies the general agreement of theory with experiment for this transition is quite reasonable in view of the somewhat imprecisely described transition density.

D. The $T=0$ states of ^{12}C

1. The 2^+ state at 4.44 MeV

The CKWF reproduce the shape of the longitudinal (e, e') form factor²⁷ $F_L(q)$ out to $q \sim 2 \text{ fm}^{-1}$ but the magnitude of the calculated $|F_L|^2$ requires an enhancement factor of 2 to match the data. The calculated $B(E2)$ for this transition requires an enhancement factor of about 1.6. On the basis of the (e, e') results the spin-independent part of the transition density should be reliable out to $q \sim 2 \text{ fm}^{-1}$, which for (p, p') at $E_p = 122$ (185) MeV corresponds to $\theta_{c.m.} \sim 50^\circ$ (45°).

As can be seen in Fig. 10 the calculated cross sections at each bombarding energy are overestimated with use of the average renormalization

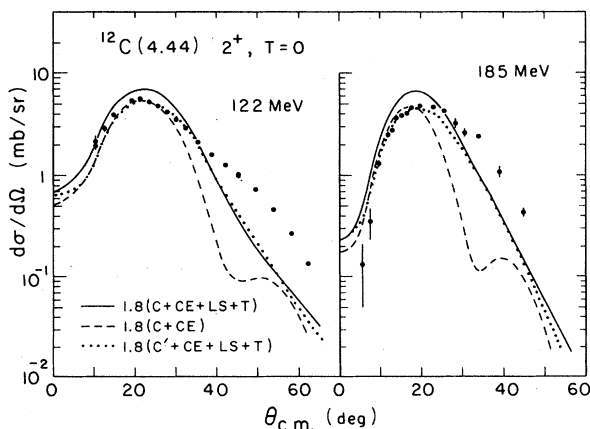


FIG. 10. Comparison of DWIA calculations with data for the 4.44-MeV transition in ^{12}C . See also the caption of Fig. 8. Coulomb excitation (CE) is included. The dotted curves are for a calculation in which the imaginary part of the central interaction was reduced by a factor of 2 (C'). The renormalization of 1.8 accounts for known core-polarization effects.

factor of 1.8. The spin-orbit part of V^{eff} is important at the larger angles and increases the integrated cross section by $\sim 60\%$ ($\sim 100\%$) at $E_p = 122$ (185) MeV. The cross sections at these larger angles are still considerably underestimated relative to the forward peak.

Indirect but independent information is available on the scalar-isoscalar part of V^{eff} from folding-model estimates of the central part of the optical potential.⁴ The real part of the volume integral (per nucleon) of the phenomenological optical potential agrees reasonably well with that of V^{eff} while the imaginary part is overestimated by about a factor of 2. For this reason calculations were also made in which the overall strength of the imaginary part of V^{eff} was reduced by a factor of 2. The shape of the calculated cross section is only slightly altered but a renormalization of it by a factor of ~ 1.8 is now required, in good agreement with the electromagnetic results. Expansion of the shell-model basis space has been found to produce good agreement for cross sections at 61 MeV without any renormalization.³²

The relatively poor shape of the calculated cross section for $q \gtrsim 1.2 \text{ fm}^{-1}$ may indicate the need for a larger $S=1$ component in the transition density. (It may be noted that the shapes of the experimental cross sections for this state and for the 16.11-MeV state, which is dominated by $S=1$, are quite similar.) The CKWF do not represent the shape of the relevant transition density $|F_T(q)|^2$ from (e, e') experiments very well and the calculated magnitude is low by a factor of 3.²⁷ Another possibility is that coupled-channels effects are beginning to show up at larger angles.²¹

2. The 1^+ state at 12.71 MeV

With an oscillator parameter chosen to reproduce the peak positions of the (e, e') transverse form factor, the CKWF underestimates $|F_T(q)|^2$ by roughly a factor of 4. An earlier (e, e') measurement of the electromagnetic width reported³³ a value of 0.35 eV which is also much larger than the value 0.113 eV given by the CKWF. The very small calculated width and form factor are due to isoscalar $M1$ suppression in self-conjugate nuclei and in addition to a cancellation of spin and orbital contributions. It makes these transitions very sensitive to isovector impurities in the wave functions.³⁰ The (p, p') reaction may be less sensitive to such impurities since the relative contributions from spin and current densities may be quite different, even though the ratio of central isovector to isoscalar coupling strengths is large and comparable to (for small momentum transfers) the analogous ratio for the (e, e') reaction. Explicit calculations based on the mixing coeffi-

cients proposed in Refs. 30 and 33 showed that the effects of isospin mixing were entirely negligible, changing the 1^+ (p, p') cross sections by 5% or less.

The CKWF are not only clearly inadequate for a satisfactory description of the electromagnetic excitation of this state, but are also inadequately tested by (e, e') data with respect to their reliability for use in (p, p') calculations. This is to be contrasted with the excitation of the $T=1$ state at 15.1 MeV which has a large $S=1$ isovector transition density (and a weak current term) so that (e, e') experiments yield a relatively reliable measure of the transition density sampled by (p, p').

Figure 11 shows a comparison between the calculated and measured (p, p') cross sections at $E_p = 122$ MeV. The experimental cross sections are not well described in the DWIA. The large and predominantly isovector tensor force, which was derived from the Sussex oscillator matrix elements and which also describes the $N-N$ t matrix reasonably well, overestimates the cross sections at small angles without reproducing the shoulder in the experimental cross section near 40° . Figure 11 also illustrates the strong sensitivity of this transition (unlike most $T=1$ transitions) to the particular representation of the tensor part of the t matrix. In particular the curve labeled $C+LS+T'$, for which the tensor interaction was obtained from a detailed fit⁴ to the momentum components ($q \lesssim 2$ fm⁻¹) of the t matrix, describes the shape of the experimental cross section quite well forward of 30° . This angle corresponds to $q \sim 1.2$ fm⁻¹, just where $|F_T(q)|^2$ has a strong minimum. The magnitude of the calculated cross section forward of 30° is, how-

ever, still too large by 50–60%.

Since the tensor force contributes primarily through the exchange terms for this state, the difference between the two tensor forces considered is likely due to their differences near $q \sim 2.2$ fm⁻¹ where the Sussex-based (“detailed fit”) tensor force is larger (smaller) than the actual $N-N$ t matrix. Except for the 2.31-MeV transition in ^{14}N , none of the other transitions considered here are particularly sensitive to the choice of tensor force in this range of momentum transfer.

Analogous calculations have been made at 185 MeV and these are compared with experimental data in Fig. 11. At this energy, where only forward angle data are available, a reasonable description of the data is obtained without renormalization. The shape of the cross section is also reasonably well reproduced, with a preference for the Sussex-based tensor force for $\theta_{c.m.} \gtrsim 15^\circ$. At smaller angles ($\theta_{c.m.} \lesssim 10^\circ$) the “detailed fit” tensor force is clearly preferred. As is seen in Fig. 11, the *shape* of the experimental cross section is given best with no tensor force; in this case the magnitude is 50% too small. The difference in normalizations required at the two energies studied here is not understood but may reflect the decreasing importance of multistep processes with increasing bombarding energy. This is discussed further in Sec. V B. The predicted asymmetries for each of the tensor forces considered here are relatively large and good data should discriminate between them.

E. The states of ^{14}N

1. The 0^+ state at 2.31 MeV

At first glance the transition to this state should be rather like that for the 15.11-MeV state in ^{12}C since the transfer quantum numbers ($S=T=1$) are the same and the same parts of V^{eff} can contribute. However, this transition is known^{34,35} to be quite sensitive to the isovector part of the tensor force and is therefore especially suitable for testing that portion of V^{eff} .

The sensitivity arises from the extremely small transition density at small momentum transfers, where the central part of V^{eff} dominates, together with the relatively greater importance of the tensor part of V^{eff} at larger momentum transfers.^{4,36} This is an essential property of any wave function that is consistent with the strongly inhibited Gamow-Teller matrix element for the analogous β decay of ^{14}C .

This property is illustrated in Fig. 12 where the quantity

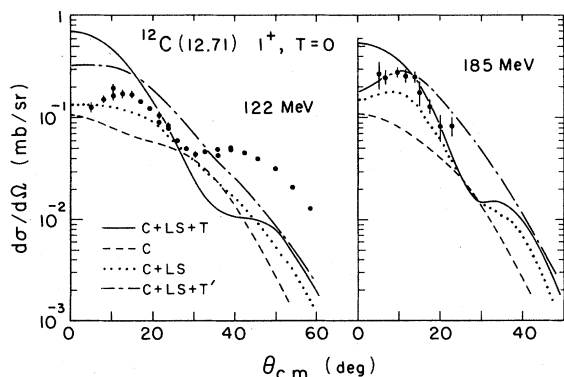


FIG. 11. Comparison of DWIA calculations and data for the 12.71-MeV transition in ^{12}C . See also the caption for Fig. 8. The dash-dot curve shows the result of a calculation that used the “detailed-fit” tensor interaction (T'). Renormalization of that curve by 0.64 would cause it to pass through most data points out to 30° .

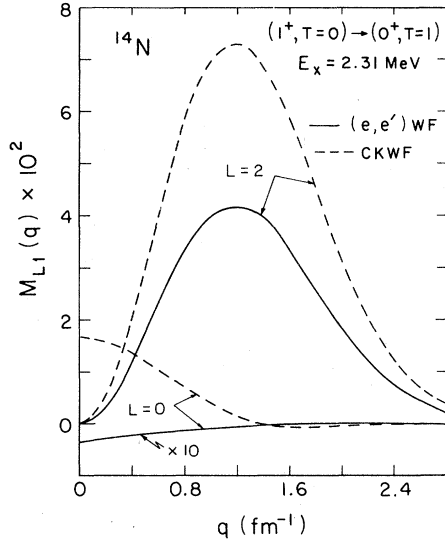


FIG. 12. The transition density in momentum space for the 2.31-MeV transition in ^{14}N . Shown are $L=0$ and 2 components for the CKWF and the wave functions given in Ref. 19. The $L=0$ component of the latter has been multiplied by an extra factor of 10.

$$M_{LJ}(q) = \left\langle J_f \left\| \sum_i j_L(g r_i) T_{L1J}(\Omega_i, \vec{\sigma}_i) \tau_{iz} \right\| J_i \right\rangle \quad (4)$$

is plotted in arbitrary units for both the CKWF and the more recent wave functions deduced from electron scattering.²⁹ The oscillator parameter of 0.588 fm^{-1} is not well determined. The tensor T_{L1J} is constructed from a spherical harmonic of rank L and a Pauli spin operator. M_{LJ} is proportional to that part of the transverse-magnetic form factor for electron scattering which may be attributed to the spin density. The amplitude for each orbital (L) and total (J) angular momentum transfer to the target in the (p, p') reaction is proportional to M_{LJ} . Here $J=1$ with $L=0, 2$. The wave functions deduced from electron scattering²⁹ (and other constraints) are seen to yield $L=0$ and $L=2$ transition densities that are considerably weaker than those of the CKWF. The latter are known to overestimate both the (e, e') cross section and the $L=0$ β -decay rate.

In Fig. 13 the (p, p') cross sections at $E_p = 122 \text{ MeV}$ are compared with DWIA calculations for each set of wave functions described above. Auxiliary calculations show that the central exchange contributions cancel about 95% of the central direct cross section and the $L=2$ transfers to the projectile³⁶ are rather small. The angular distribution at this stage is relatively flat out to about $30\text{--}35^\circ$. Interference with the tensor force produces the minimum in the $15\text{--}20^\circ$ region. Near $\theta_{c.m.} \sim 30^\circ$ ($q \approx 1.3 \text{ fm}^{-1}$) the contribution of the ten-

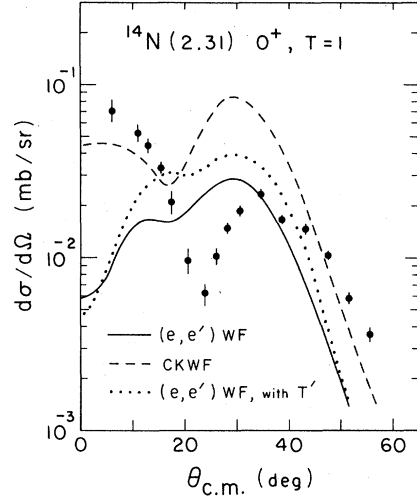


FIG. 13. Comparison of DWIA calculations and data for the 2.31-MeV transition in ^{14}N . See also the captions for Figs. 8, 11, and 12.

sor force is roughly 5 times that of the central force. Although none of the results are very satisfactory, the magnitude of the second peak is only given correctly when the wave functions constrained by (e, e') are used. This is a direct consequence of the relative sizes of $M_{21}(q)$ for the two sets of wave functions.

At this point it should be stressed that the (e, e') data²⁹ on which the (e, e') wave functions are based only cover momentum transfers corresponding (in the plane-wave approximation) to scattering angles between $\sim 15^\circ$ and $\sim 30^\circ$, a region where, on the basis of the above calculation for the 1^+ state ^{12}C at 15.11 MeV , the $N\text{--}N$ effective interaction used here appears adequate. Unlike the transition in ^{12}C which is dominated at small q by a relatively large $L=0, S=1$ transition density, contributions from multistep processes cannot be ruled out for this weak transition in ^{14}N , particularly for small q where matrix elements involving the nuclear current dominate. That this may in fact be so is discussed in Sec. VB.

There is also noticeable sensitivity to the tensor terms as is shown by the curve in Fig. 13 for the (e, e') wave functions and the "detailed fit" tensor interaction. Unfortunately, the possible interference with multistep processes makes a preferred choice here somewhat difficult.

The inhibition of small-momentum transfers suggests that in using this reaction to test effective forces, relatively greater emphasis should be placed on describing the second maximum. It is worth noting that this maximum appears at a constant momentum transfer $1.5 \pm 0.1 \text{ fm}^{-1}$ and has a constant cross section $22 \pm 2 \mu\text{b/sr}$ over the

range of bombarding energies 30–122 MeV.³⁷ One may suggest the need for additional (e, e') data for this state out to somewhat larger momentum transfers ($q \gtrsim 2 \text{ fm}^{-1}$) in order to define the magnitude of the transition density over the peak more precisely.

Effects of admixtures from the $2s-1d$ shell were studied by using the extended CKWF (CKSD) given in Tables I and III of Ref. 38. The vanishing Gamow-Teller β -decay matrix element is achieved with these wave functions by strong cancellation between the p -shell and sd -shell contributions so that $M_{01}(q)$ is much smaller for small q than given by the CKWF; the $M_{21}(q)$ for the CKSD is, however, very similar in shape but 0.86 times the size of that for the CKWF. The calculated (p, p') cross section using the CKSD is almost identical in shape to that obtained by using the (e, e') wave functions but is ~ 2.3 times as large at the peak. This accurately reflects the peak values of the corresponding $M_{21}(q)$ but still yields a poor description of the data.

2. The 1^+ state at 3.95 MeV

This transition is perhaps the most complicated of all. Since it is between two 1^+ states, three J transfers are allowed. However, the $J=2$ contribution is much larger than that for $J=1$ and the $J=0$ contribution is negligible. Both the V_0 and V_σ parts of the V^{eff} can contribute, as well as the V_{LS} and V_{Ten} terms.

The $J=2$ transition density is roughly 30% larger for $S=1$ than for $S=0$. This is in sharp contrast with the excitation of the $2^+ T=0$ state in ^{12}C at 4.44 MeV where the CKWF give an $S=1$ transition density that is negligible compared to that for $S=0$. The situation is reminiscent of the 16.11-MeV transition in ^{12}C . An important difference, however, is that the ^{14}N transition is isoscalar and V_σ is much weaker than V_0 so that sensitivity to the $S=1$ transition density is not very large. In summary, then, the 3.95-MeV transition in ^{14}N might be expected to be reasonably similar to the 4.44-MeV transition in ^{12}C .

Empirically, the peak cross sections for these two states imply $B(E2)\uparrow = 3.5 e^2 \text{ fm}^4$ for the ^{14}N transition, based on a value¹⁷ $B(E2)\uparrow = 39 e^2 \text{ fm}^4$ for the 4.44-MeV transition in ^{12}C . The recent (e, e') experiment of Ensslin *et al.*²⁹ yielded $B(E2)\uparrow = 3.4 \pm 0.3 e^2 \text{ fm}^4$ for ^{14}N . An independent lifetime measurement,³⁹ together with known $M1/E2$ mixing ratios and branching ratios,⁴⁰ resulted in a value $3.3 \pm 0.2 e^2 \text{ fm}^4$. The CKWF used here give $B(E2)\uparrow = 1.7 e^2 \text{ fm}^4$ so that an upward renormalization of the (p, p') calculations by a value of about 2 is expected.

In Fig. 14 an enhancement of the calculated cross

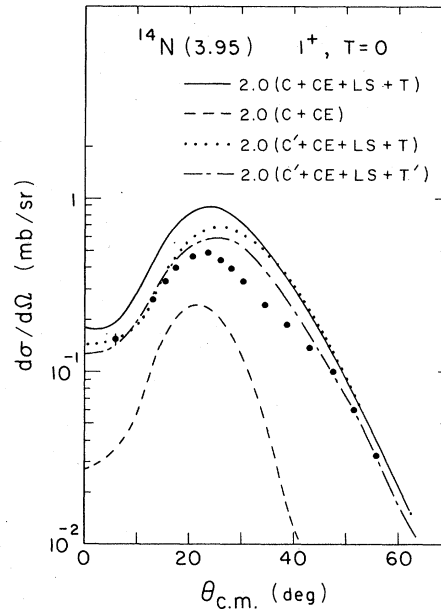


FIG. 14. Comparison of DWIA calculations and data for the 3.95-MeV transition in ^{14}N . See also the captions for Figs. 8, 10, and 11.

section (solid curve) by only 10% would have been required to match the experimental cross section. The shape of the angular distribution is reasonably well reproduced. Just as for the 4.44-MeV state in ^{12}C , calculations have also been made in which the imaginary coupling was reduced by a factor of 2. The shape of the calculated cross section is slightly worse, but the magnitude is in better agreement with the data.

The dashed curve in Fig. 14 shows the calculated cross section when the “detailed fit” tensor force is used and the imaginary coupling is also reduced by a factor of 2. This gives the best agreement of all. Until the $S=1, J=2$ part of the transition density and the large-momentum components of the tensor force are better understood it is difficult to draw more definitive conclusions. An (e, e') measurement of the transverse $E2$ form factor could in principle give more precise information on the $S=1$ part of the transition density, but this would likely be dominated by the $M1$ component.

V. ADDITIONAL CONSIDERATIONS

A. Simpler approaches

The magnitude and complexity of the calculations in Sec. IV raise the question whether a simpler approach might be possible. It has already been made clear that accurate wave functions are essential. Indeed it is the purpose of such studies eventually to learn more details about nuclear wave functions. Since the exact treatment of knockon

exchange is the most time-consuming part of these calculations, it might be hoped that an appropriate pseudopotential for use in conventional computer programs might be sufficiently accurate. Such approaches are also necessary for investigating the importance of more complex reaction mechanisms.

Following Austin,³⁴ it is attractive to consider a simple $N-N$ interaction consisting of a real, central interaction with a Yukawa radial dependence having a range of 1 fm. The strengths and volume integrals needed to fit the cross sections of the four states of ^{12}C discussed in Sec. IV are listed in Table III. The CK wave functions were used. The calculated curves were normalized to the data for the best overall visual agreement for angles less than about 35° . The fits are quite satisfactory in this range for all but the 12.71-MeV state. The calculated curve for this resembles the solid curve in Fig. 11 and it was normalized similarly.

For comparison a Gaussian radial dependence $\sim \exp(-r^2/b^2)$ with $b = 1.8$ fm was also tried. This value of the range parameter produces about the same mean-square radii as the Yukawa interaction. The calculated angular distributions for the 2^+ states peak at 20° and fall off more rapidly than for the Yukawa case so the fitting was confined to smaller angles. The interaction strengths are again listed in Table III.

Unfortunately, while this approach is useful at lower energies, it is of dubious validity here. It has been shown that the spin-orbit and tensor parts of the $N-N$ interaction are quite important at intermediate energies for most of these transitions so that the phenomenological extraction of strengths is subject to much uncertainty. Furthermore, no Yukawa or Gaussian form with a single range can come close to reproducing the shape of the 12.71-MeV transition. Even in zero range, the calculated curve decreased much too steeply at forward angles. Sophisticated treatments of the radial dependence are therefore essential.

TABLE III. Strengths (MeV) of a simple 1-fm Yukawa or 1.8-fm Gaussian interaction for inelastic proton scattering to states of ^{12}C . Volume integrals in units MeVfm^3 are given in parentheses. Core-polarization enhancement factors (see Sec. IV) have not been factored from the numbers.

Term	Excitation energy	Yukawa	Gaussian
V_0	4.44	45 (570)	18 (580)
V_σ	12.71	~ 14 (180)	~ 6 (190)
V_τ	16.11	17 (210)	6.7 (210)
$V_{\sigma\tau}$	15.11	14 (180)	6.0 (190)

It might be possible, however, to use the microscopic interaction described in Sec. IV in computer codes that do not evaluate the exchange contributions exactly and to use an appropriate pseudopotential^{4, 41, 42} for these. To explore this issue many of the above calculations were repeated with the programs DWUCK4 and CHUCK3.⁴³ The exchange pseudopotential was available only for the central part of V^{eff} . The tensor interaction was also slightly different from that in Sec. IV since these programs use a regularized OPEP form. Neither program has a microscopic $\vec{L} \cdot \vec{S}$ interaction, although DWUCK4 had been modified to handle a deformed-spin-orbit coupling potential in the Oak Ridge form.⁴⁴

In general this approach was moderately successful. It became clear though that no shortcuts were possible. Both the even and odd parts of the two-body interaction were necessary, as were also the exchange pseudopotential, the imaginary parts of the form factors, the tensor interaction, and all L and S transfers. In specific cases some of these ingredients were not too important, but it is hard to know these cases in advance.

The best representation was for the 15.11-MeV transition in ^{12}C . Here the imaginary form factor was small. The exchange terms reduced the cross section due to the central direct terms by about an order of magnitude, reflecting the inclusion of odd-state forces. The tensor terms fine tuned the shape by allowing projectile $L = 2$ amplitudes to contribute slightly. With everything included the calculations were nearly identical to the results of the DWBA70 program. It thus seems that such an approach may be feasible for transitions dominated by the OPE process. Even the 2.31-MeV transition in ^{14}N was reproduced nearly perfectly for angles $> 20^\circ$. At smaller angles, the dip near 15° was deeper and the 0° cross section was larger.

The situation was not so good for the 2^+ excitations in ^{12}C . Also, the worst case was the 12.71-MeV isoscalar spin-flip transition. Here the final cross sections were an order of magnitude below the DWBA70 calculations, although the angular dependence was similar. It is difficult to assess the reasons for the difficulties. It is known, however, that the exchange contributions of the tensor interaction are frequently very important. They could not be included in these alternate calculations.

Since a microscopic $\vec{L} \cdot \vec{S}$ interaction was not available in these programs, consideration was given to the use of a collective spin-orbit coupling potential. Figure 15 shows a comparison of central and spin-orbit cross sections for the $2^+ T = 0$ state of ^{12}C as calculated with the collective and microscopic models. The deformed spin-orbit potential

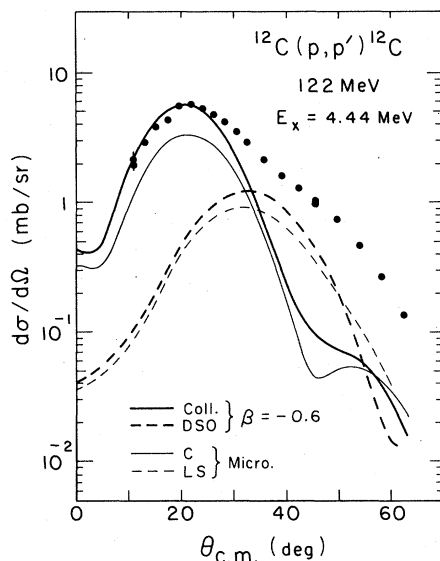


FIG. 15. Results of collective-model and microscopic-model calculations of the cross sections for the central and spin-orbit contributions to the excitation of the 4.44-MeV state in ^{12}C . A deformation parameter $\beta = -0.6$ was used for the collective model.

was of the full Thomas form. The Oak Ridge form⁴⁴ produced a distinctively different shape and the combined result was rather less satisfactory.

It should be stressed that all comparisons were made with respect to cross sections. The moderate success in this regard does not extend to polarizations. For these the full treatment, with the $\vec{L} \cdot \vec{S}$ interaction, is essential.

B. Multistep processes

A final concern in the comparison of theory with experiment is the possibility of multistep processes. It is argued in Ref. 21 that, at intermediate energies, an optical potential that fits proton elastic-scattering data embodies many effects of the couplings to other channels. Nevertheless, individual features of some multistep processes may still remain.

Two types of multistep processes were considered. In the first case, cross sections for the 1^+ states in ^{12}C were computed for excitations that proceeded through the strong 2^+ $T=0$ state. The CKWF were used throughout and the amplitude for the $0^+ \rightarrow 2^+$ step was renormalized in order to match the experimental cross sections. Also, the V_0 interaction for the $2^+ \rightarrow 1^+$ ($T=0$) step was adjusted to increase the cross sections by compensating for the deficiency noted in Sec. V A. These calculations produced at most 4 and 2 $\mu\text{b/sr}$ at 0° for the 12.71- and 15.11-MeV states, respectively, several orders of magnitude below the data.

The second case dealt with pickup-stripping

processes through the states of ^{11}C or ^{13}N . The CKWF were used for all spectroscopic amplitudes. A folded potential of the Johnson-Soper type⁴⁵ was used for the deuteron channels, with parameters based on the energy systematics²¹ of proton scattering from ^{12}C . These zero-range calculations included the common correction terms for non-locality and finite range with parameters selected in accordance with exact finite-range calculations of the $^{12}\text{C}(p, d)^{11}\text{C}$ ground-state transition. Even though experimental cross sections⁴⁶ for the (p, d) reaction were reproduced well, there is no assurance that the two-step calculations have the correct magnitude. Quite possibly they are overestimated due to finite-range and nonorthogonality effects.⁴⁷

The shapes of the (p, d, p) two-step cross sections at 122 MeV were typically peaked at 0° and fell off fairly rapidly with angle, much like one-step (p, d) cross sections. There was generally a fair amount of cancellation among the paths through different intermediate states (three states in ^{11}C and five in ^{13}N). Maximum cross sections of about 60, 100, and 70 $\mu\text{b/sr}$ were found for the states at 12.71, 15.11, and 16.11 MeV in ^{12}C , respectively, with these being at 0° for the 1^+ states and 23° for the 2^+ state. For ^{14}N the maximum two-step cross section was about 15 $\mu\text{b/sr}$ for angles less than 20° .

It is clear that while the two-step cross sections are not large, they could be important for the 12.71- and 2.31-MeV transitions. These are the ones described least well by the DWIA calculations. Even the 2^+ $T=1$ state in ^{12}C may not be free of concern. Since the transition amplitudes computed by the DWBA70 program are in a different (i.e., helicity) convention from that of CHUCK3, interference effects have not been explored in detail. Preliminary studies with the one-step amplitudes as represented by CHUCK3 indicate that some improvements in fitting the data are possible. Uncertainties about the details of the (p, d, p) calculations as well as about the accuracy of the complex phases in the CHUCK3 representation of the one-step paths preclude further conclusions at this time.

VI. SUMMARY AND CONCLUSIONS

The DWIA calculations of the $^{12}\text{C}(p, p')^{12}\text{C}$ cross sections are based on several implicit experimental constraints: (a) The effective t matrix is taken from phase-shift fits to N - N scattering data; (b) the shell-model effective interaction is determined by fitting to experimental energy levels; (c) the optical-model parameters are determined by fitting proton elastic-scattering

data; (d) bound-state harmonic-oscillator parameters are determined from (e, e') data of longitudinal and transverse form factors; and (e) renormalizations have been made to correct for known deficiencies of the shell-model wave functions. Within this environment the calculations have no adjustable parameters. The comparisons with data are remarkably good and satisfying, particularly over the range of momentum transfer where the wave functions are in good accord with electron-scattering form factors. Apart from known deficiencies (see Sec. IVD1), the impulse approximation seems to work rather well.

The best agreement occurs for the $V_{\sigma\tau}$ part of V^{eff} , which is dominated by the OPE process, at least for momentum transfers $q \leq 1.5 \text{ fm}^{-1}$. The V_0 and tensor parts also seem to be described fairly well. The enhancement factor required to match the data for the $2^+ T=0$ state of ^{12}C is related primarily to the truncation of the shell-model space to the $1p$ shell,³² although there is good reason to believe that the imaginary part of V_0 is too large. The tensor terms of the effective interaction plays an important role in the excitation of the 16.11-MeV state in ^{12}C and the 2.31-MeV state in ^{14}N . In both cases there are also important contributions from other terms and some uncertainty about the precise wave functions.

The study here does not shed much light on the V_τ and V_σ interactions. The former might be expected to be most important for the 16.11-MeV transition, but it turns out that, with the CKWF, the $S=1$ transition density and $V_{\sigma\tau}$ terms dominate. It appears, however, not to be far from correct. The coordinate-space representation of the $S=1$, $T=0$ two-body interaction is poorly determined and is quite noisy. The volume integral of the real part is quite small and its mean square radius is

negative.⁴ The calculations for the 12.71-MeV state in ^{12}C are not very satisfactory, although there is substantial sensitivity to the tensor force and probably also to (p, d, p) multistep contributions.

It is unfortunate that knockon exchange is still an important consideration at these energies. Calculations that use a pseudopotential were moderately successful for cross sections but not for polarization quantities. The exchange contributions should decrease at higher energies and it is possible that the tensor and spin-orbit terms may eventually decrease also.

Additional (e, e') data for large q would be very beneficial in order to provide a more thorough foundation for the (p, p') calculations. Also (p, p') data on ^{12}C and ^{14}N in the 200–400 MeV range would provide a basis for useful extensions of techniques described here. There is some reason to hope that multistep processes²¹ and exchange terms will be less important there and that the sensitivity to the ingredients of V^{eff} will be more direct. If so, our knowledge and understanding of effective interactions should be enriched considerably.

ACKNOWLEDGMENTS

This work was supported in part by the National Science Foundation under Grants Nos. PHY76-84033, PHY76-23468, PHY77-24134, and PHY78-22696. Additional support for computations was provided by the University of Georgia, the University of Pittsburgh, and Oak Ridge National Laboratory. We are indebted to F. Petrovich for helpful discussions regarding the electron scattering, to the University of Massachusetts electron-scattering group for providing numerical values of the (e, e') form factors, and to J. B. McGrory for providing the CKWF in a convenient form.

*Present address: Indiana University Cyclotron Facility, Bloomington, Ind. 47401.

¹J. P. Jeukenne, A. Lejeune, and C. Mahaux, *Phys. Rep.* **25C**, 83 (1976); *Phys. Rev. C* **16**, 80 (1977).

²F. A. Brieva and J. R. Rook, *Nucl. Phys.* **A291**, 299, 317 (1977); **A297**, 206 (1978); **A307**, 493 (1978).

³G. Bertsch, J. Borysowicz, H. McManus, and W. G. Love, *Nucl. Phys.* **A284**, 399 (1977).

⁴W. G. Love, in *Proceedings of the Conference on (p, n) Reactions and the Nucleon-Nucleon Force, Telluride, Colorado, 1979*, edited by C. D. Goodman, S. M. Austin, S. T. Bloom, J. R. Rapaport, and G. R. Satchler (Plenum, New York, 1980), p. 23.

⁵J. R. Comfort, in *Proceedings of INS International Symposium on Nuclear Direct Reaction Mechanism, Fu-kuoka, Japan, 1978*, edited by M. Tanifuji and K. Yazaki (INS, University of Tokyo, 1979), p. 118.

⁶K. A. Amos, H. V. Geramb, R. Sprickmann, J. Arvieux,

M. Buenerd, and G. Perrin, *Phys. Lett.* **52B**, 138 (1974).

⁷A. K. Kerman, H. McManus, and R. M. Thaler, *Ann. Phys. (N.Y.)* **8**, 551 (1959).

⁸D. Hasselgren, P. U. Renberg, O. Sundberg, and G. Tibell, *Nucl. Phys.* **69**, 81 (1965).

⁹A. Ingemarsson, O. Jonsson, and A. Hallgren, *Nucl. Phys.* **A319**, 377 (1979).

¹⁰R. M. Haybron and H. McManus, *Phys. Rev.* **136**, B1730 (1964).

¹¹R. M. Haybron, M. B. Johnson, and R. J. Metzger, *Phys. Rev.* **156**, 1136 (1967).

¹²H. K. Lee and H. McManus, *Phys. Rev.* **161**, 1087 (1967).

¹³M. Buenerd, *Phys. Rev. C* **13**, 444 (1976).

¹⁴V. C. Officer, R. S. Henderson, and I. D. Svalbe, *Bull. Am. Phys. Soc.* **20**, 1169 (1975).

¹⁵R. Kouzes and A. Broad, I.U.C.F. Internal Report No. 75-6 (unpublished).

- ¹⁶P. Schwandt, private communication.
- ¹⁷F. Ajzenberg-Selove, Nucl. Phys. A248, 1 (1975).
- ¹⁸M. Buenerd, P. Martin, P. deSaintignon, and J. M. Loiseaux, Nucl. Phys. A286, 377 (1977).
- ¹⁹K. T. Knöpfle, G. J. Wagner, A. Kiss, M. Rogge, C. Mayer-Böricke, and Th. Bauer, Phys. Lett. 64B, 263 (1976).
- ²⁰See AIP document No. PAPS PRVCA 21-2147-20 for 20 pages of differential cross-section data. Order by PAPS number and journal reference from American Institute of Physics, Physics Auxiliary Publications Service, 335 East 45th Street, New York, New York 10017. The price is \$1.50 for microfiche or \$5.00 for photocopies. Airmail is additional. Make checks payable to the American Institute of Physics.
- ²¹J. R. Comfort and B. C. Karp, Phys. Rev. C 21, 2162 (1980).
- ²²G. R. Satchler, Nucl. Phys. A100, 481 497 (1967).
- ²³W. G. Love, A. Scott, F. T. Baker, W. P. Jones, and J. D. Wiggins, Jr., Phys. Letters 73B, 277 (1978).
- ²⁴M. H. MacGregor, R. A. Arndt, and R. M. Wright, Phys. Rev. 182, 1714 (1969).
- ²⁵A. Picklesimer and G. E. Walker, Phys. Rev. C 17, 237 (1978).
- ²⁶R. Schaeffer and J. Raynal (unpublished).
- ²⁷J. B. Flanz, R. S. Hicks, R. A. Lindgren, G. A. Peterson, A. Hotta, B. Parker, and R. C. York, Phys. Rev. Lett. 41, 1642 (1978) and references therein; G. A. Peterson and R. A. Lindgren, private communication.
- ²⁸S. Cohen and D. Kurath, Nucl. Phys. 73, 1 (1965).
- ²⁹N. Ensslin, W. Bertozzi, S. Kowalski, C. P. Sargent, W. Turchinets, C. F. Williamson, S. P. Fivozinsky, J. W. Lightbody, Jr., and S. Penner, Phys. Rev. C 9, 1705 (1974).
- ³⁰E. G. Adelberger, R. E. Marrs, K. A. Snover, and J. E. Bussolletti, Phys. Rev. C 15, 484 (1977).
- ³¹A. Friebel, P. Manakos, A. Richter, E. Spamer, W. Stock, and O. Titze, Nucl. Phys. A294, 129 (1978).
- ³²K. Amos and I. Morrison, Phys. Rev. C19, 2108 (1979).
- ³³F. E. Cecil, L. W. Fagg, W. L. Bendel, and E. C. Jones, Jr., Phys. Rev. C 9, 798 (1974).
- ³⁴S. M. Austin, in *The Two-Body Force in Nuclei*, edited by S. M. Austin and G. M. Crawley (Plenum, New York, 1972), p. 285. See also Ref. 4, p. 203.
- ³⁵G. M. Crawley, S. M. Austin, W. Benenson, V. A. Madsen, F. A. Schmittroth, and M. J. Stomp, Phys. Lett. 32B, 92 (1970).
- ³⁶W. G. Love and L. J. Parish, Nucl. Phys. A157, 625 (1970).
- ³⁷Sam M. Austin and S. H. Fox, in *Proceedings of the International Conference on Nuclear Physics, Munich, Germany*, edited by J. deBoer and H. J. Mang (North-Holland, Amsterdam, 1973), Vol. I, p. 388.
- ³⁸H. J. Rose, O. Häusser, and E. K. Warburton, Rev. Mod. Phys. 40, 591 (1968).
- ³⁹M. Bister, A. Anttila, and J. Keinonen, Phys. Rev. C 16, 1303 (1977).
- ⁴⁰J. W. Olness, A. R. Poletti, and E. K. Warburton, Phys. Rev. 154, 971 (1967).
- ⁴¹F. Petrovich, H. McManus, V. A. Madsen, and J. Atkinson, Phys. Rev. Lett. 22, 895 (1969).
- ⁴²W. G. Love, Nucl. Phys. A312, 160 (1978).
- ⁴³P. D. Kunz (unpublished); extended versions of J. R. Comfort.
- ⁴⁴M. P. Fricke, R. M. Drisko, R. H. Bassel, E. E. Gross, B. J. Morton, and A. Zucker, Phys. Rev. Lett. 16, 746 (1966).
- ⁴⁵R. C. Johnson and P. J. R. Soper, Phys. Rev. C 1, 976 (1970).
- ⁴⁶J. R. Shepard, R. E. Anderson, J. J. Kraushaar, and J. R. Comfort (unpublished).
- ⁴⁷P. D. Kunz and L. A. Charlton, Phys. Lett. 61B, 1 (1976).